

Final Report

D.O.E. (Contract EY-76-S-02-2766.A002)

The Dynamics of Relativistic e-Beam Diodes

June 1, 1978 - May 31, 1979

I. INTRODUCTION

We have studied the reflex diode both with and without a prepulse plasma filling the anode-cathode gap and have found at least qualitative agreement with the 1-d theory.<sup>1,2</sup> The prepulse plasma causes the diode to operate in a low impedance mode throughout the pulse with no early high impedance phase normally associated with the reflex diode.<sup>2,3</sup> In addition we have made some preliminary investigations of the 2-d characteristics of the reflex mode using x-ray pinhole photography from bremsstrahlung emission at the anode foil. Studies of prepulse plasmas on high  $\nu/\gamma$  pinch diodes have also been conducted.

II. EFFECT OF PREPULSE PLASMA FILL ON THE REFLEX DIODE

The diode shown in schematic view in Fig. 1 consisted of a steel needle cathode and a thin foil anode of aluminized mylar. The aluminized side of the foil faced the cathode. Foil thickness varied from 0.5 mil to 3.0 mil and the entire diode was immersed in a 9.2 kG magnetic field. The cathode was coated with a thin layer of carbon on shots when the laser was used to produce a carbon prepulse plasma. The 1.5J CO<sub>2</sub> laser was incident on the tip of the cathode and was fired sufficiently early to allow a carbon plasma plume of density approximately  $10^{15} \text{ cm}^{-3}$  to completely fill the diode.

**NOTICE**

This report was prepared as an account of work sponsored by the United States Government. Neither the United States nor the United States Department of Energy, nor any of their employees, nor any of their contractors, subcontractors, or their employees, makes any warranty, express or implied, or assumes any legal liability or responsibility for the accuracy, completeness or usefulness of any information, apparatus, product or process disclosed, or represents that its use would not infringe privately owned rights.

## **DISCLAIMER**

**This report was prepared as an account of work sponsored by an agency of the United States Government. Neither the United States Government nor any agency Thereof, nor any of their employees, makes any warranty, express or implied, or assumes any legal liability or responsibility for the accuracy, completeness, or usefulness of any information, apparatus, product, or process disclosed, or represents that its use would not infringe privately owned rights. Reference herein to any specific commercial product, process, or service by trade name, trademark, manufacturer, or otherwise does not necessarily constitute or imply its endorsement, recommendation, or favoring by the United States Government or any agency thereof. The views and opinions of authors expressed herein do not necessarily state or reflect those of the United States Government or any agency thereof.**

## **DISCLAIMER**

**Portions of this document may be illegible in electronic image products. Images are produced from the best available original document.**

Examples of current and voltage traces from the normal reflex diode and the plasma filled reflex diode are shown in Figs. 2 and 3. For the case of no laser-produced plasma in Fig. 2, the voltage is seen to rise to 350kV for the early part of the pulse and operates at an impedance greater than  $20\Omega$ . After 25nsec the voltage drops sharply and plateaus at about 50kV until plasma closure shorts the diode late in the shot. During this voltage plateau the impedance of the diode falls to about  $1\Omega$  and very high current densities are observed.

Simple 1-d reflex theory predicts that once the electrons start reflexing the high currents generated drag down the diode voltage due to internal generator resistance. As the diode voltage falls, the electron range in the foil  $R_o$  and hence the average number of transits through the foil  $\eta$  decreases. A steady state is predicted when  $\eta$  becomes a few transits.<sup>2</sup>

In Fig. 4 we plot plateau voltage versus foil thickness  $\tau$ . The solid line is a contour of constant  $R_o/\tau$  taken from electron range data.<sup>4</sup> The average number of transits  $\eta$  should scale roughly as  $R_o/\tau$ . For foils less than 1.5 mill thick the plateau voltage increases with  $\tau$  so as to keep  $\eta$  constant as predicted by theory. For thicker foils the plateau voltage deviates somewhat from the constant  $\eta$  curve. It does appear, however, that the diode is operating in the reflex mode once the voltage has dropped to the plateau value. The plateau voltage was independent of anode-cathode gap spacing  $d$  but the time required for the voltage to drop increases with  $d$  as is shown in Fig. 5.

When the laser was fired at the cathode tip producing a pre-pulse plasma in the diode, the current and voltage traces looked

like the example in Fig. 3. The diode voltage immediately plateaus and the current rises at a 25% greater rate than the non-laser case. The plateau voltage versus foil thickness for this case is also plotted in Fig. 4 and is seen to agree closely with those values measured with no prepulse plasma present.

The effect of the prepulse plasma is, therefore, to cause the diode to go immediately into low impedance operation without the initial high impedance phase. This may be important for several reasons. In short pulse machines an appreciable amount of the available energy is lost during the high impedance phase. The presence of the prepulse plasma seems to speed the reflexing process and more efficiently couple energy into reflexing. Secondly, during the high impedance phase of the reflex diode pulse most of the pulse energy is reflected back into the generator due to impedance mismatch at the diode. On large machines the resulting damage can be quite severe. The ability to eliminate this high impedance mode may be important if high voltage, low impedance machines are coupled to reflex diodes.

### III. 2-d OBSERVATIONS OF THE REFLEX DIODE

We have made some investigations of the 2-d properties of the reflex diode described earlier in this report. The principal diagnostics in these studies were 2 x-ray pinhole cameras whose locations are shown in Fig. 1. Camera #1 was located directly behind the anode looking along the diode axis. Camera #2 was located beside the cathode looking back into the anode-cathode gap almost perpendicular to the diode axis. Both cameras had  $x1$  magnification and were located outside the vacuum system with 10 mill mylar vac-

uum windows the only disturbance in the x-ray optical path. The effective pinhole diameter measured for both camera and found to be 0.12mm. A typical x-ray picture from Camera #2 is shown in Fig. 6. There is an area of intense x-ray emission 0.65mm across and less intense wings which measure 9mm across. The pictures from Camera #1 are simply circular spots whose diameters are slightly less than that of the intense emission area seen in Camera #2.

In Fig. 7 the spot diameter as measured by Camera #1 is plotted versus the anode-cathode gap spacing for a variety of conditions. For solid aluminum anodes of  $\tau=3$ mm the spot decimeter increases linearly with  $d$ . For the thin foil anodes  $\tau=0.5$  mil the spot decimeter increases much more slowly with  $d$  and seems to be unaffected by the magnetic field. The only effect of eliminating the magnetic field was a slight increase in current accompanied by an increase in the size of the wings measured by Camera #2. This is attributed to enhanced emission from the sides of the cathode needle.

In Fig. 8 spot diameter is plotted versus thickness for two different gap spacings. A slight rise in spot diameter with  $\tau$  is noted and the increase in spot diameter with  $d$  as seen in the previous figure is retained.

Pinhole photography for the plasma-filled reflex diode was attempted but the softness of the bremsstrahlung x-rays, due to the diode voltages, caused high absorption in air and in the 10 mil mylar vacuum windows. The resulting low photon flux caused difficulty in obtaining good x-ray pictures from this diode.

#### IV. EFFECT OF PARTIAL PLASMA FILL ON THE PINCH DIODE

The diode used in these experiments is shown in Fig. 9. It consisted of a carbon-coated annular cathode with a 4mm inside diameter. The  $\text{CO}_2$  laser described earlier was focused through this hole incident onto the anode. The anode consisted, typically, of 1/8" thick aluminum. In order to allow the laser to pass through the cathode the marx was run in reverse polarity with the cathode at ground potential. An x-ray pinhole camera was imbedded in the anode shank to observe bremsstrahlung emission.

One of the principal variables in this experiment was the anode-cathode gap spacing  $d$ . This spacing is known to close in time due to motion of the high density anode and cathode plasmas. The closure velocity was measured as shown in Fig. 10 and found to be  $4.6 \times 10^6 \text{ cm/sec.}$

We observed pinching in the absence of the laser-produced anode plasma as a function of the corrected gap spacing as shown in Fig. 11. Peak current appropriately normalized by parapotential theory is plotted against the reciprocal of the corrected gap width. The gaps in which pinching was observed, as determined by anode damage, are shown as circular points. They are observed to fall on a straight line as parapotential theory predicts.<sup>5</sup> At large anode-cathode gaps (triangle data points) pinching is not observed and the data does not exhibit this linear behavior.

In Fig. 12 peak current over voltage to the  $3/2$  power is plotted against the inverse square of the corrected gap spacing for the unpinched data. The data is seen to be linear in accord with Child-Langmuir space charge limited flow. It is seen, therefore, that for sufficiently small anode-cathode gaps the diode operates

in a pinched mode; however, for large anode-cathode gaps the critical current for pinching is not obtained and the diode exhibits space charge limited flow.

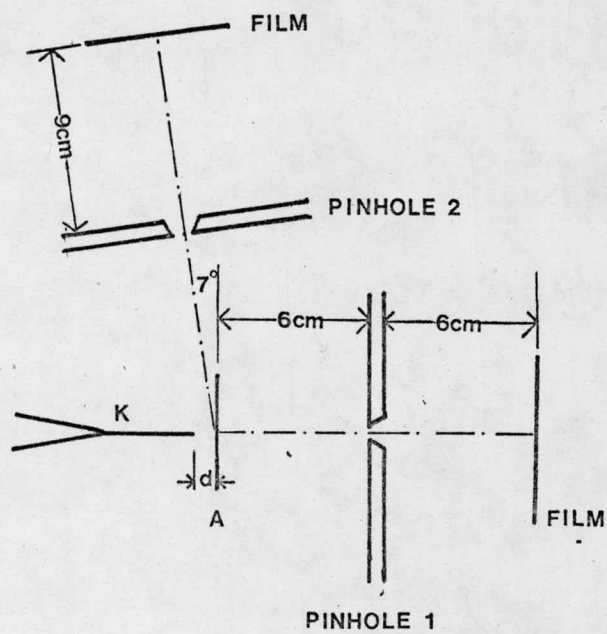
In conducting experiments with the laser-produced anode plasma present we operated at an anode-cathode gap of 2.55 mm which exhibited unpinched flow in the absence of any laser plasma. The laser was fired almost coincidently with the voltage pulse partially filling the gap with plasma. Pinching was observed in these shots as can be seen in Fig. 13. The anode on the left is from a shot with no laser plasma present. There is broad low-level surface damage with no evidence of pinching. The anode on the right is from a shot with the laser-produced anode plasma present. There is localized high-level damage indicative of pinching.

The presence of the laser-anode plasma, therefore, caused the diode to pinch at values of  $d$  which had exhibited unpinched flow. This may be simply due to a smaller effective gap which allows the space charge limited current to exceed the critical current for pinching or to the effect that the laser plasma has on ion flow from the anode.

G. Bekefi

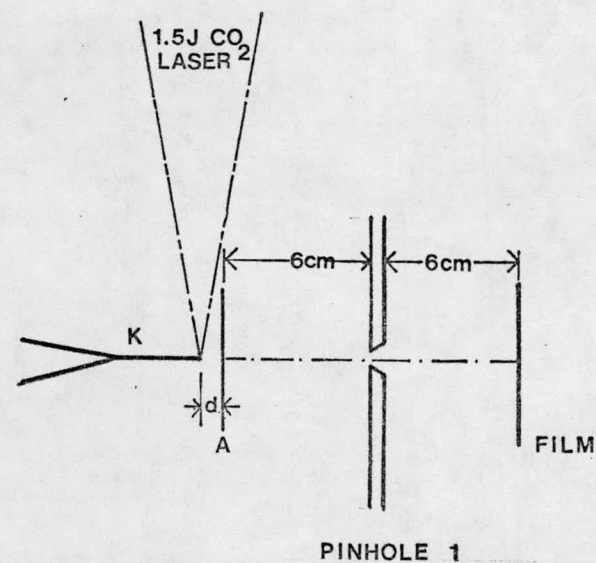
REFERENCES

1. D.S. Prono, J. M. Creedan, I. Smith, and N. Bergstron, *J. Appl. Phys.* 46, 3310 (1975).
2. A. Sternlieb, Shyke A. Goldstein, and R. Lee, University of Maryland Plasma Preprint PL #79-D10 (1979).
3. G. Cooperstein, S. Goldstein, J.J. Condon, D. Hinshelwood, D. Mosher, S. J. Stephanakis, *Bull. Am. Phys. Soc.* 23, 800 (1978).
4. S. M. Seltzer and M. J. Berger, *Nucl. Instr. Methods* 119, 157 (1974).
5. J. M. Creedan, *J. Appl. Phys.* 46, 2946 (1975).



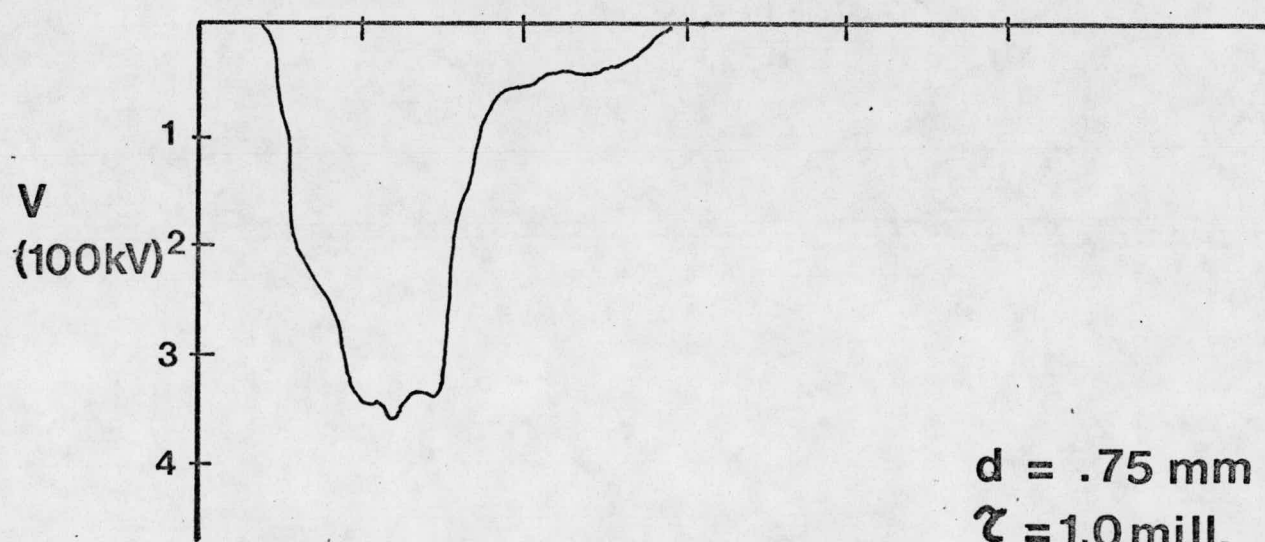
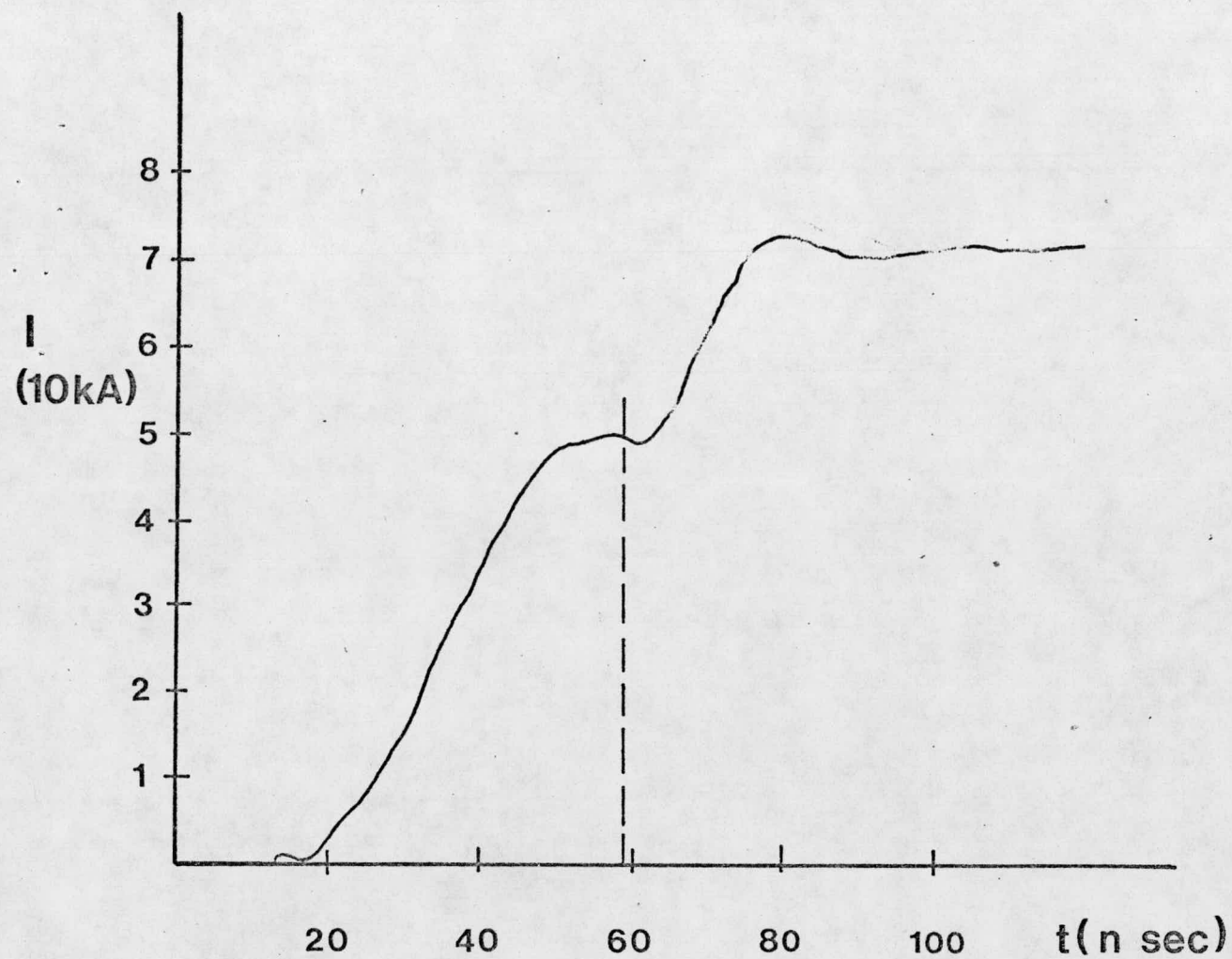
SIDE VIEW

DIODE SCHEMATIC



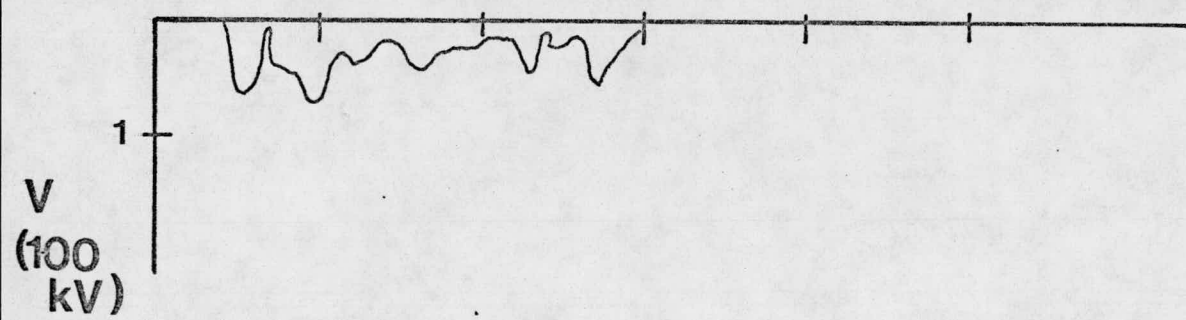
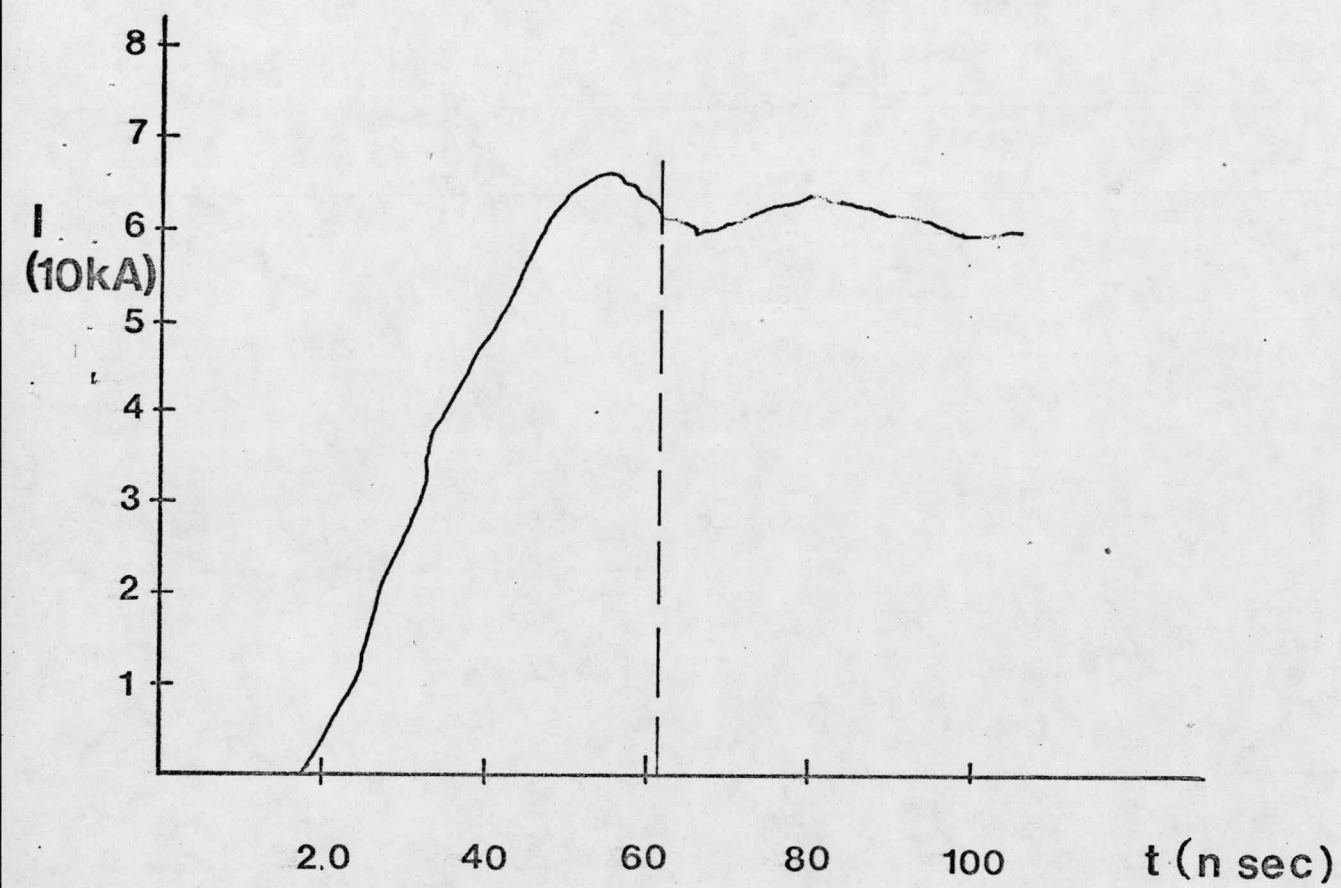
TOP VIEW

Fig. 1



$d = .75 \text{ mm}$   
 $\tau = 1.0 \text{ mill.}$

Fig. 2



$d = .75 \text{ mm}$   
 $\gamma = .5 \text{ mill. Laser on}$

Fig. 3

### PLATEAU VOLTAGE VS. FOIL THICKNESS

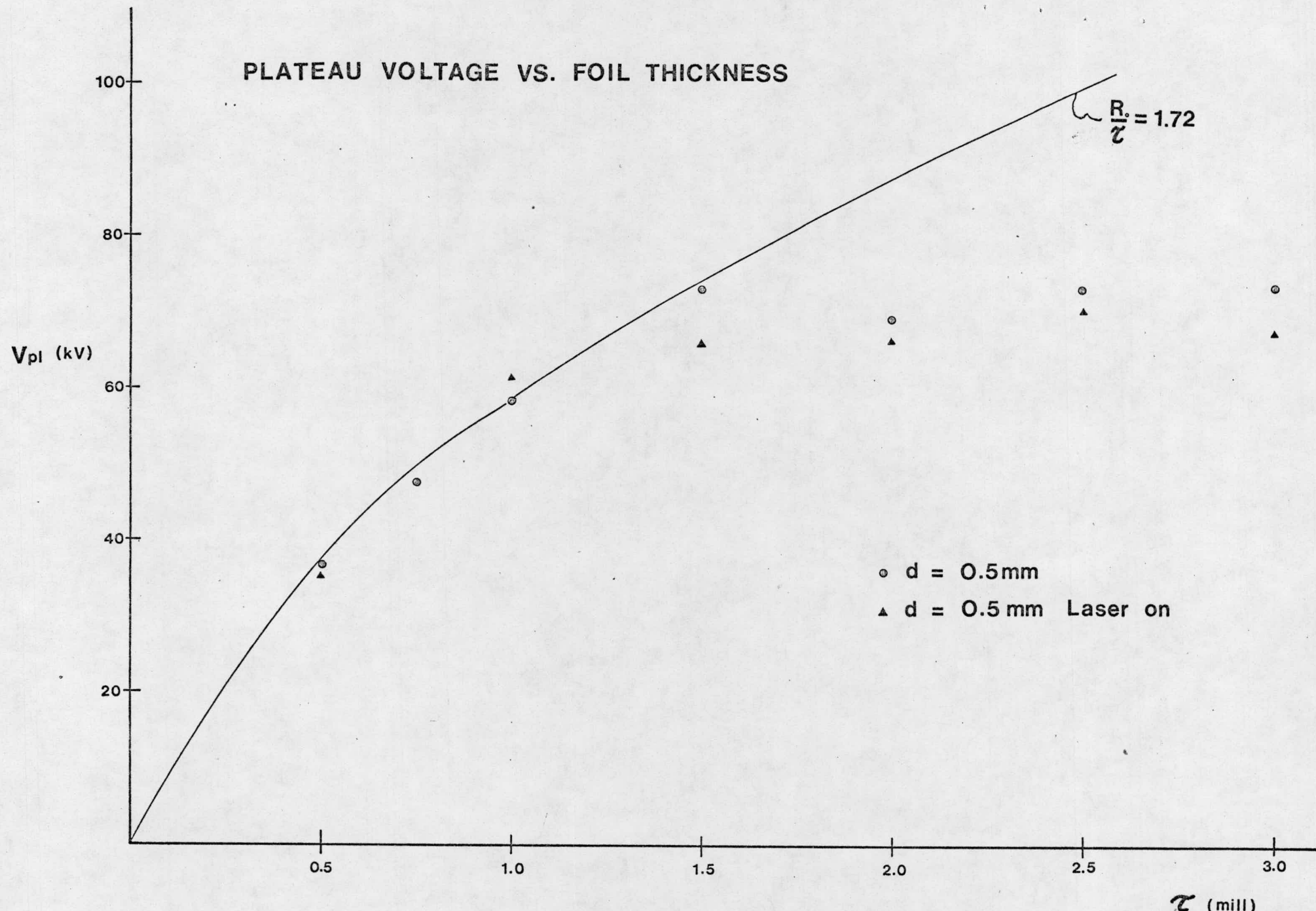


Fig. 4

## TIME TO PLATEAU VS GAP SPACING

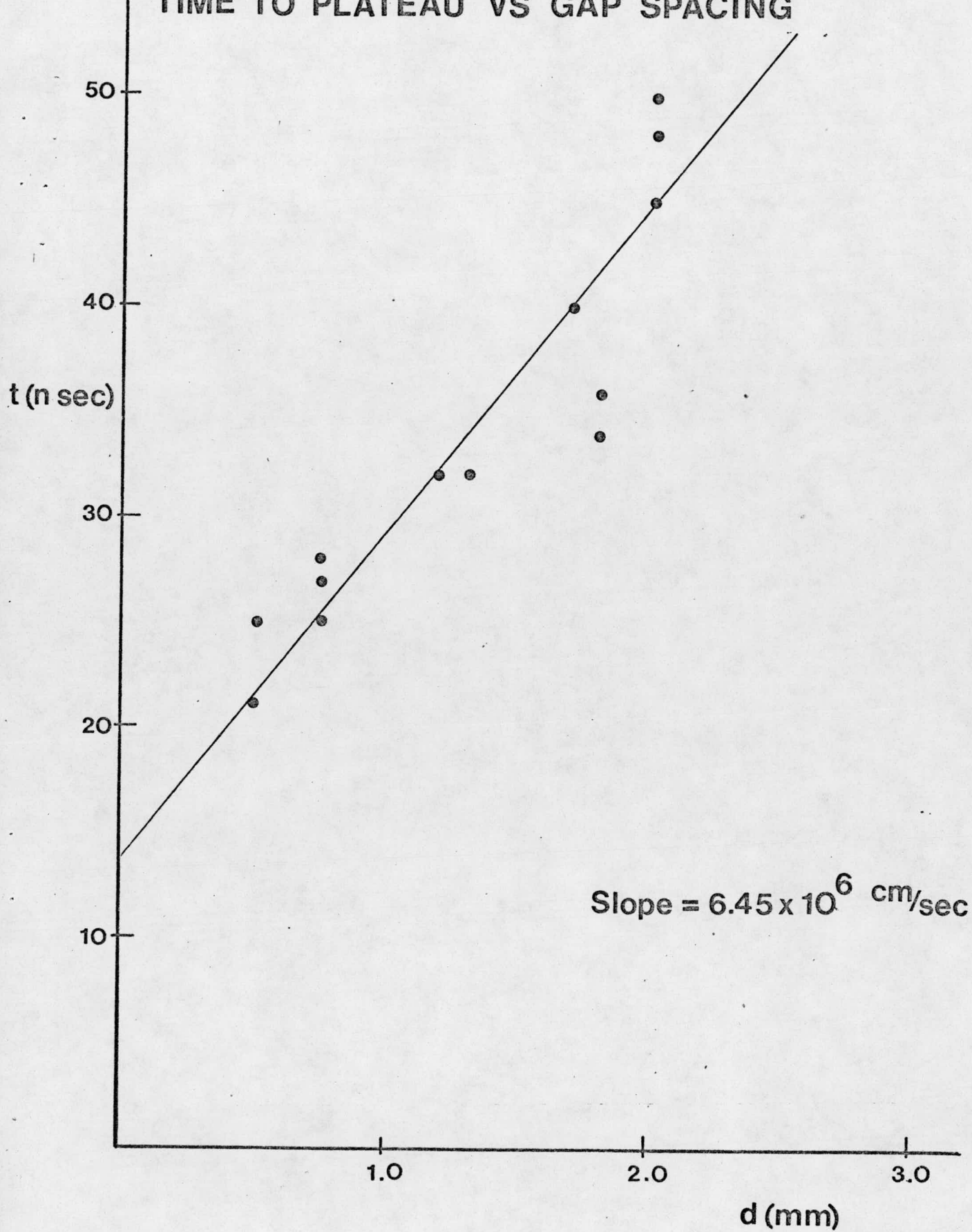


Fig. 5

Fig. 6

## SPOT DIAMETER VS. GAP SPACING

D  
mm)

5

4

3

2

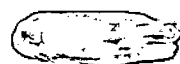
1

1.0

2.0

3.0

d(mm)



•  $\tau = 3.0$  mm

△  $\tau = .5$  mill B = 9.2 kG

▲  $\tau = .5$  mill B = 0

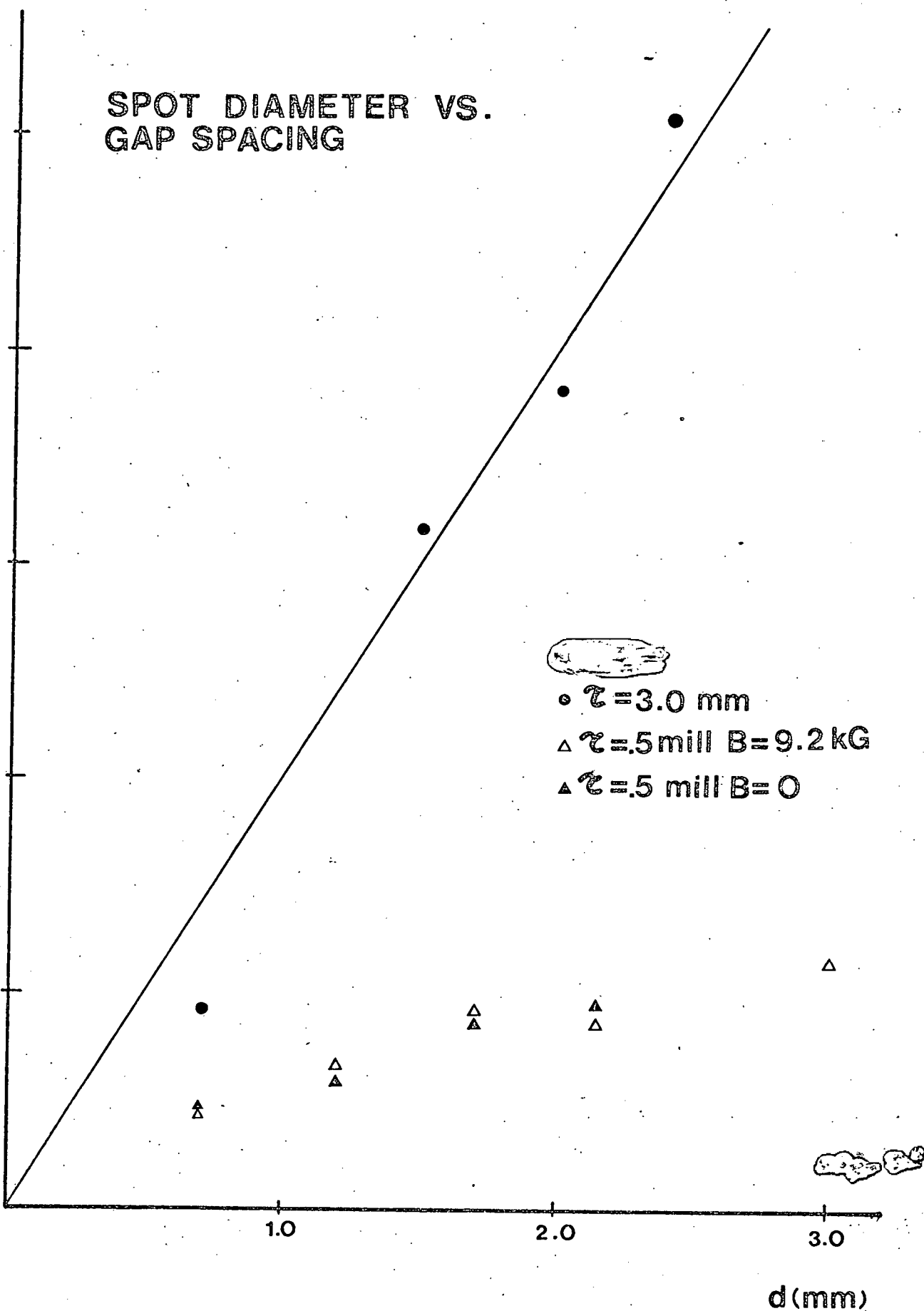


Fig. 7

## SPOT DIAMETER VS FOIL THICKNESS

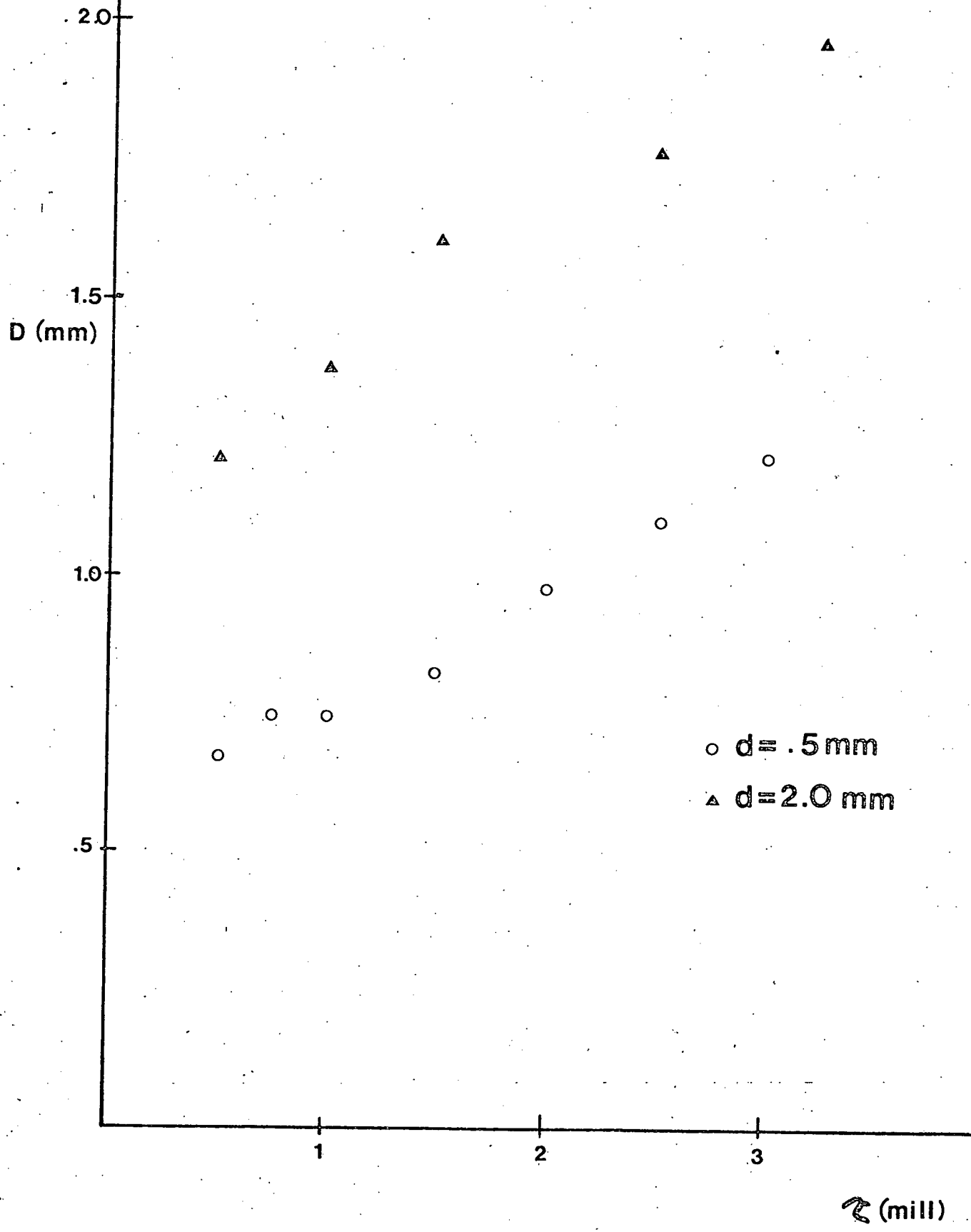
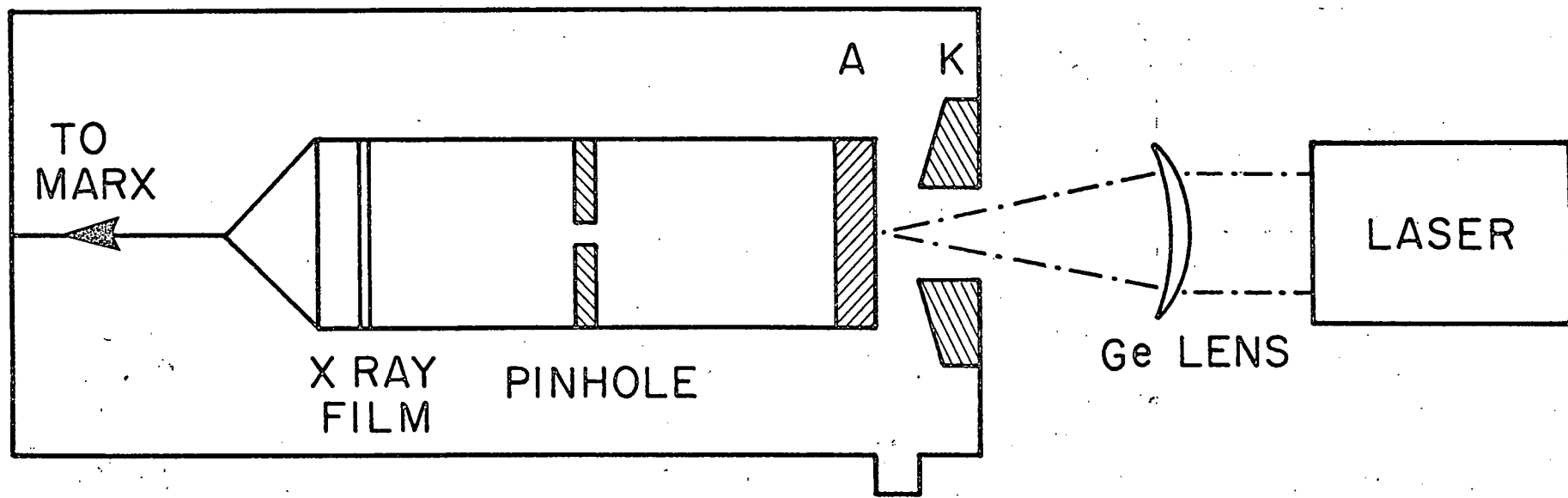


Fig. 8



SCHEMATIC OF EXPERIMENTAL SETUP

Fig. 9

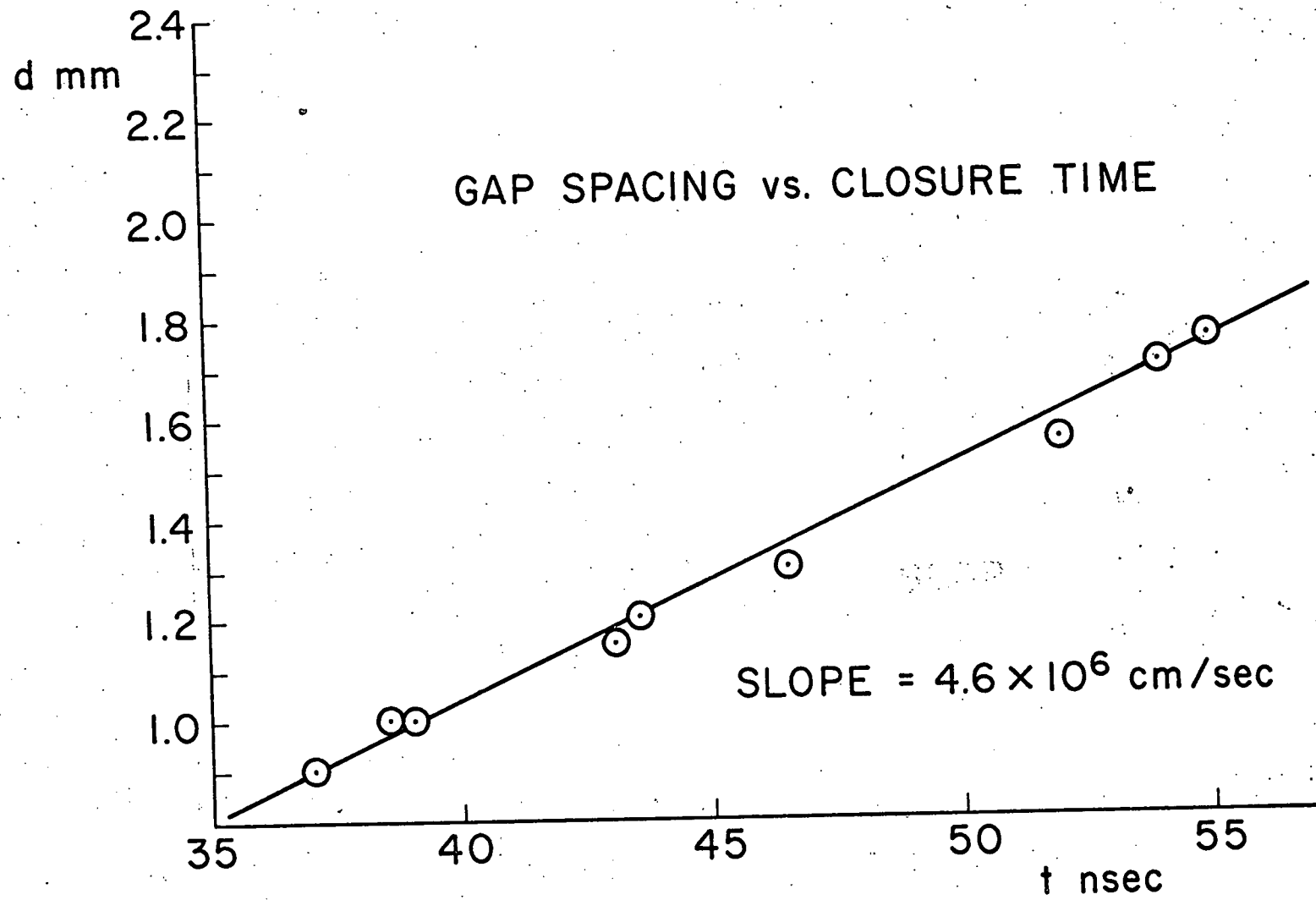


Fig. 10

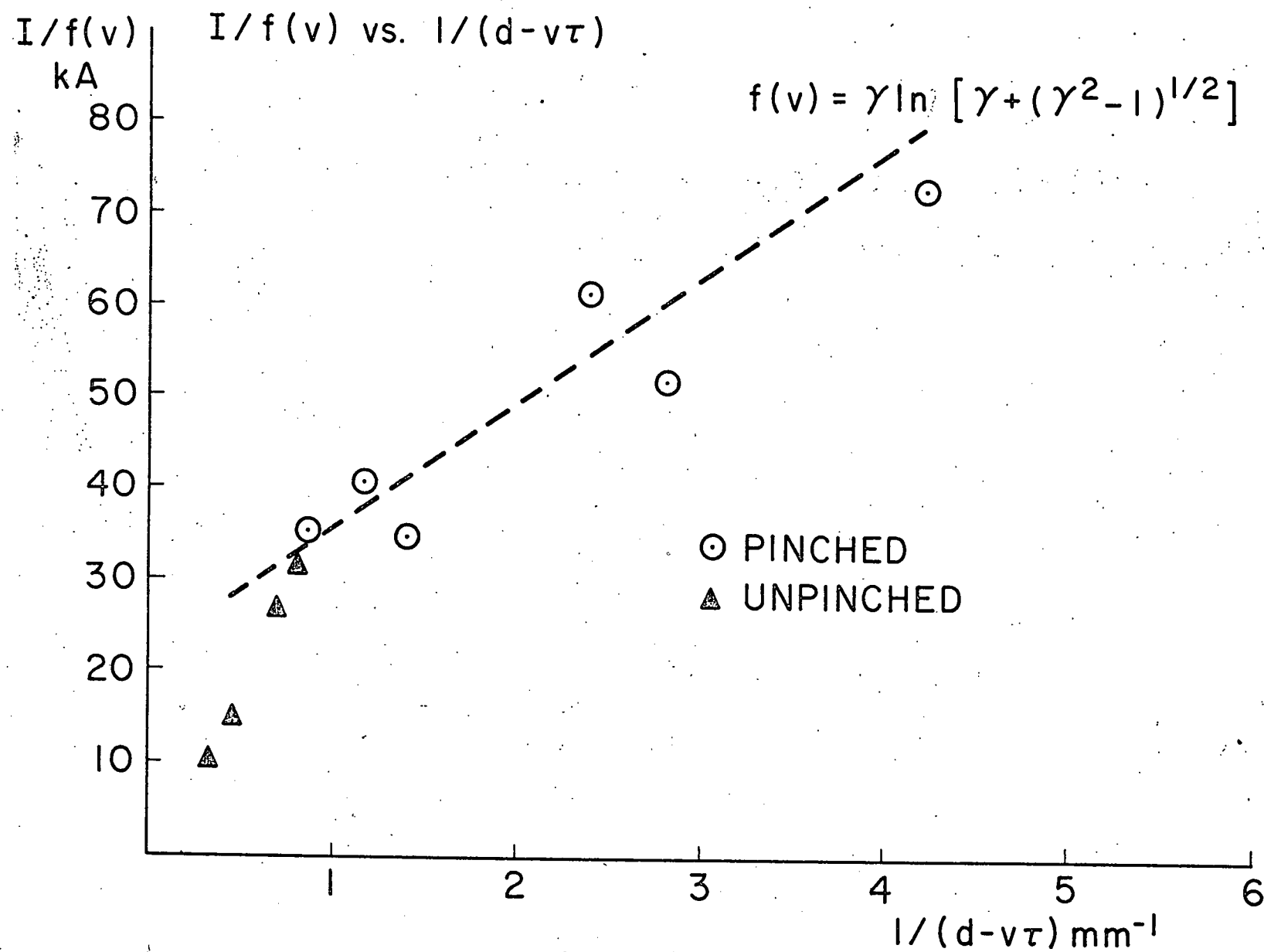


Fig. 11

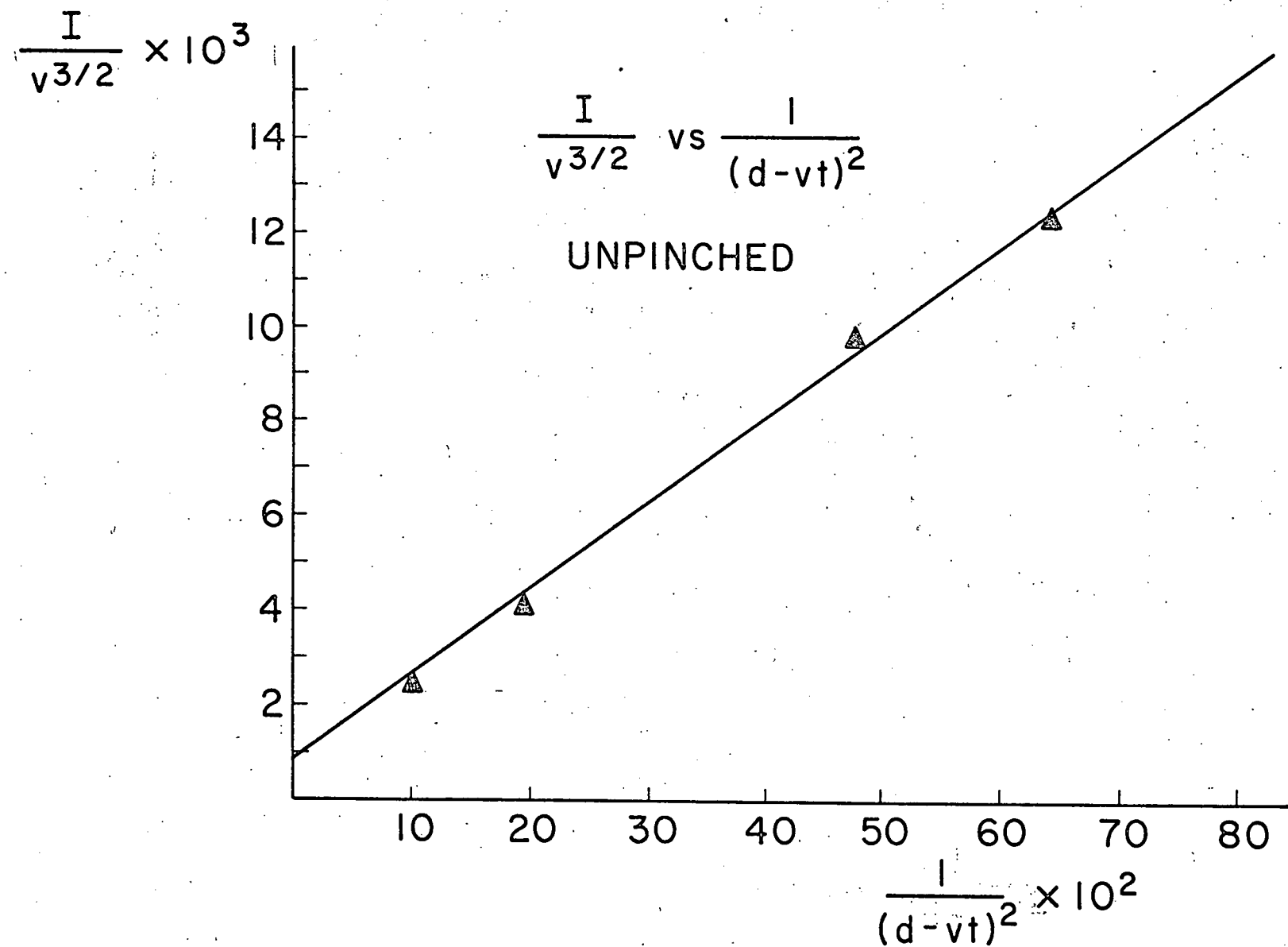


Fig. 12

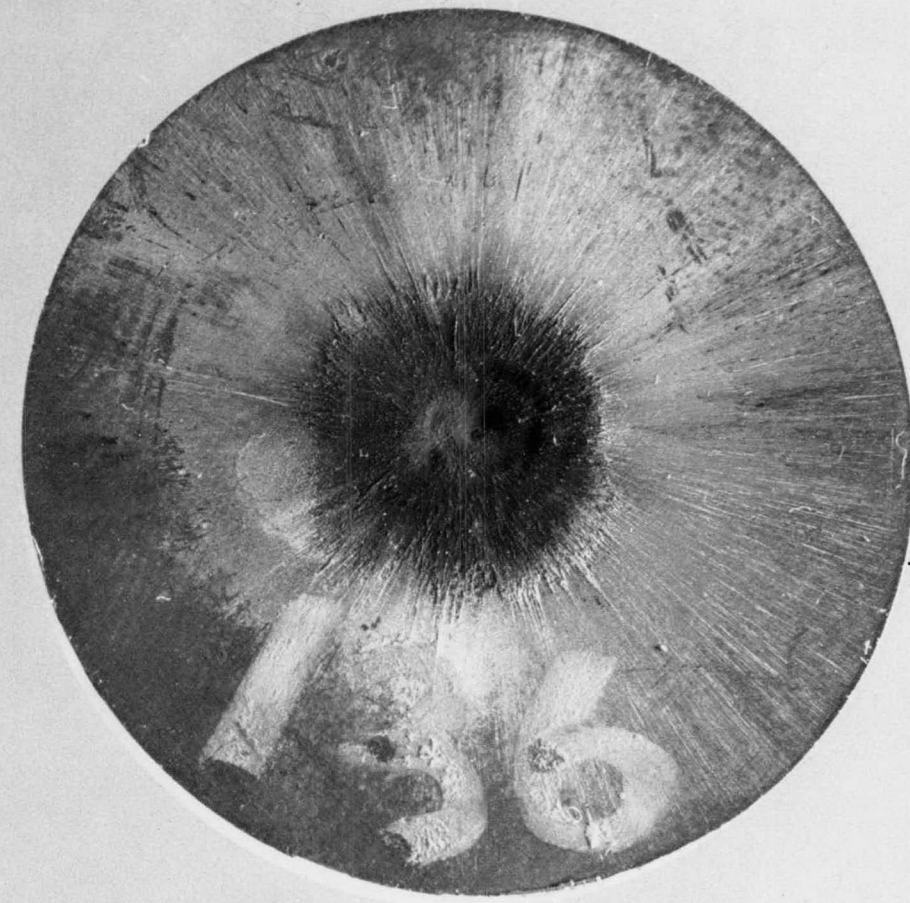
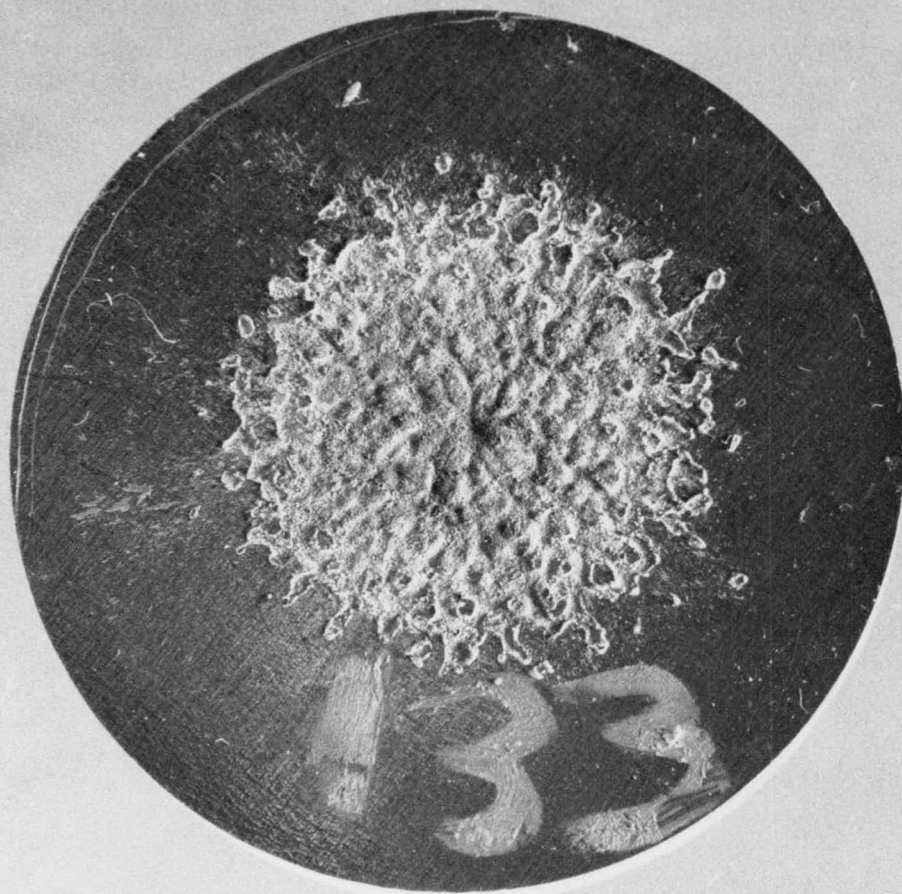


Fig. 13